Interaction of Lipophilic Ions with the Plasma Membrane of Mammalian Cells Studied by Electrorotation

Markus Kürschner, Katja Nielsen, Christian Andersen, Vladimir L. Sukhorukov, Wolfdieter A. Schenk, Roland Benz, and Ulrich Zimmermann

Lehrstuhl für Biotechnologie, Biozentrum and Institut für Anorganische Chemie der Universität Würzburg, Am Hubland, D-97074 Würzburg, Germany

ABSTRACT The electrical properties of biological and artificial membranes were studied in the presence of a number of negatively charged tungsten carbonyl complexes, such as $[W(CO)_5(CN)]^-$, $[W(CO)_5(NCS)]^-$, $[W_2(CO)_{10}(CN)]^-$, and $[W(CO)_5(SCH_2C_6H_5)]^-$, using the single-cell electrorotation and the charge-pulse relaxation techniques. Most of the negatively charged tungsten complexes were able to introduce mobile charges into the membranes, as judged from electrorotation spectra and relaxation experiments. This means that the tungsten derivatives act as lipophilic anions. They greatly contributed to the polarizability of the membranes and led to a marked dielectric dispersion (frequency dependence of the membrane capacitance and conductance). The increment and characteristic frequency of the dispersion reflect the structure, environment, and mobility of the charged probe molecule in electrorotation experiments with biological membranes. The partition coefficients and the translocation rate constants derived from the electrorotation spectra of cells agreed well with the corresponding data obtained from charge-pulse experiments on artificial lipid bilayers.

INTRODUCTION

Mobile and gating charges are a common feature of biological membranes. Mobile charges within the plasma membrane are involved in ion carrier systems (Zimmermann et al., 1982; Benz and Zimmermann, 1983; Wang et al., 1997a) and can play a role in intercellular communication (Turin et al., 1991). Their concentration in biological membranes can be markedly increased because of the partition of organic lipid-soluble ions, such as dipicrylamine (DPA^-) and derivatives of tetraphenylborate ($TPhB^-$), etc., into the membranes (Benz et al., 1976; Läuger et al., 1981; Benz and Nonner, 1981; Dilger and Benz, 1985). The permeation of lipophilic anions through artificial lipid bilayers is used as a widespread model system for ion transport phenomena in biological and artificial membranes (Cafiso and Hubbell, 1982; Honold and Stark, 1984; Benz et al., 1984; Demura et al., 1985; Arnold et al., 1988; Nolan and Voorheis, 1991; Sukhorukov and Zimmermann, 1996). Numerous studies using time- and frequency-domain techniques (charge-pulse, voltage-clamp, impedance, etc.) have demonstrated that lipophilic ions contribute greatly to the electrical polarizability of a lipid bilayer membrane (Ketterer et al., 1971; Lebedev and Boguslavsky, 1971; Wulf et al., 1977; Benz and Nonner, 1981; Pickar and Brown, 1983). The polarizability is reflected by an increase of the membrane capacitance at low frequencies and is dependent on the structure and mobility of the charged molecules. This means also that lipophilic anions adsorbed to a membrane can be used as field-sensitive molecular probes, which yield information about the structural properties of the membrane. On the other hand, the kinetics of the transport of lipophilic ions across model membranes (liposomes, lipid bilayers) offers valuable insight into the relationships between the molecular structure of the lipid-soluble molecule and its membrane permeability (Läuger et al., 1981; Benz, 1988; Hladky, 1992).

Although lipophilic anions have been widely used as experimental tools in studies of living cells and cell organelles (Oberhauser and Fernandez, 1995; Klodos et al., 1995; Lu et al., 1995; Bühler et al., 1991; Turin et al., 1991; Lichtenberg et al., 1988; Demura et al., 1985), relatively little is known about the transport of lipophilic ions in biological membranes. This is because the microelectrode methods traditionally used in electrophysiological studies (Zimmermann et al., 1982; Wang et al., 1994b, 1997a) are restricted to cells of sufficiently large size, and to frequencies below 100 kHz because of the high impedance of microelectrodes.

An alternative approach to the study of the interaction between lipophilic ions and biological membranes is the single-cell electrorotation technique (Arnold and Zimmermann, 1982). This technique represents a noninvasive method and allows the study of the ion transport kinetics in the plasma membrane of most small cells (>1–$2\ \mu m$). The technique covers a broad-band frequency window (from a few hertz to several hundred megahertz) and therefore enables the investigation of a wide time range of processes. It provides valuable information on the electrical properties of the major structural units of cells (the plasma and nuclear membrane, cytoplasm, cell wall, etc.) (Arnold et al., 1985; Sukhorukov et al., 1994; Gimsa et al., 1996; Fuhr et al., 1996). However, it must be noted that both electrorotational

Received for publication 30 December 1997 and in final form 3 March 1998.

Address reprint requests to Dr. Vladimir L. Sukhorukov, Lehrstuhl für Biotechnologie, Biozentrum der Universität Würzburg, Am Hubland, D-97074, Würzburg, Germany. Tel.: 49-0931-888-4511; Fax: 49-0931-888-4509; E-mail: biot018@rzbox.uni-wuerzburg.de.

0006-3495/98/06/3031/13 $2.00

and electrophysiological measurements of living cells can be hindered by the extreme toxicity of some organic lipophilic ions (e.g., the highly toxic environmental pollutant PCP^-; Smetjek and Wang, 1991) associated with their accumulation in the membrane and possible alteration of the membrane structure and function, caused by uncoupling of ATP synthesis or an increase in membrane permeability.

Recently, tungsten carbonyl salts have been found to increase markedly the electrical polarizability of the plasma membrane of mammalian cells over a frequency range of up to several kilohertz (Nielsen et al., 1996). In the present study, the influence of the structure of eight tungsten carbonyl anions on their adsorption to and translocation across the plasma membrane of mammalian cells was investigated in detail by means of electrorotation. From the experiments their partition coefficients and translocation rate constants in biological membranes were derived. In parallel experiments, the interaction of the lipophilic anions with artificial lipid bilayers was studied by the charge-pulse relaxation technique (Benz, 1988). Most of the tungsten carbonyl salts are reasonably soluble in water, and their cytotoxicity was found to be fairly low, which contrasts with the relatively high toxicity of large organic anions, such as the halogen-substituted derivatives of $TPhB^-$ analogs (Arnold et al., 1988).

MATERIALS AND METHODS

Chemicals

DPA^- (dipicrylamine; 2,2′,4,4′,6,6′-hexanitrodiphenylamine) (Fluka, Buchs, Switzerland) was added (at a final concentration of 1–40 μM) from an ethanol stock (1 mM) solution. The concentration of DPA^- was determined spectrophotometrically (Lambda 2 UV/VIS; Perkin-Elmer, Beaconsfield, Buckinghamshire, England), using a molar extinction coefficient of $\epsilon_{412} = 2.6 \times 10^4\ M^{-1}\ cm^{-1}$ (Wulf et al., 1977). The salts NaCl, NaCN, sodium tetraphenylborate ($TPhB^-$, $Na[B(C_6H_5)_4]$), potassium hexacyanoferrate(II) ($K_4[Fe(CN)_6] \cdot 3H_2O$), and sodium pentacyanonitrosylferrate(II) ($Na_2[Fe(CN)_5NO] \cdot H_2O$) were obtained from Merck (Darmstadt, Germany), and KSCN was from Grüssing (Filsungen, Germany). Tetraethylammonium chloride, tetraethylammonium bromide, tetraphenylphosphonium chloride ($TPhP^+$, $[P(C_6H_5)_4]Cl$), and tungsten hexacarbonyl were all obtained from Sigma (Deisenhofen, Germany).

Charge-pulse measurements on lipid bilayer membranes

Black lipid bilayer membranes were formed from a 1% solution of dioleylphosphatidylcholine (DOPC) (Avanti Polar Lipids, Alabaster, AL) in *n*-decane (Fluka). The membranes were formed across circular 1–2-mm-diameter holes in the wall separating two aqueous compartments containing 1 M NaCl in a Teflon cell. The tungsten carbonyl compounds were added to the aqueous phase in concentrated (10^{-4} to 10^{-2} M) solutions in ethanol to obtain final concentrations in the aqueous solutions between 3×10^{-8} and 3×10^{-5} M. These concentrations were chosen to obtain a linear relationship between the concentrations of the lipophilic ions in the aqueous phase and in the membrane (Benz et al., 1976; Wulf et al., 1977).

To reach partition equilibrium for the adsorption of the different lipophilic ions to the bilayers, all kinetic experiments were carried out at least 10 min after the membranes had turned completely black. The charge pulse experiments were carried out as described previously, by applying short current pulses of 5–10 ns duration to the membranes (Benz et al., 1976). In brief: one Ag/AgCl electrode was connected to a fast commercial pulse generator (Philips PM 5712) through a fast diode (reverse resistance $> 10^{11}\ \Omega$), and the other electrode was grounded. A resistor of 0.01 MΩ was introduced between the two electrodes to define a passive RC-time constant for the membrane. The voltage between these two electrodes was measured with a fast high-input-resistance voltage amplifier (bandwidth 200 MHz) based on a Burr Brown operational amplifier and a digital storage oscilloscope (Nicolet 4094). The voltage relaxations were analyzed with a 486 personal computer. They could always be fitted to two exponential relaxations with sufficient accuracy.

Cells

Mouse myeloma Sp2/0-Ag14 cells (hereafter named Sp2) were cultured in complete RPMI 1640 growth medium at 37°C under 5% CO_2 (for details, see Sukhorukov et al., 1993). Every 2–3 days, the cell suspensions were diluted 1:10 with growth medium to keep the cells in the log phase. Electrorotation measurements were performed on cells 1 day after such a 1:10 "split." Before electrorotation, Sp2 cells were washed one to three times with 150 mOsm inositol solutions (Sigma) in the absence of lipophilic compounds. After resuspension of the cell pellet in 150 mOsm inositol solution (at a final cell density of $1–2 \times 10^5$ cells/ml), the tungsten carbonyl compounds (Fig. 1; or DPA^- or other chemicals tested here) were added to the cell suspension at final concentrations of 0.1–50 μM (see Results), and the conductivity was adjusted to 1–200 mS m^{-1} by the addition of the appropriate amounts of 150 mOsm HEPES-KOH (pH 7.4) (Sigma). To reach partition equilibrium for the adsorption of the different lipophilic ions to the cell membranes, the cells were incubated with the anions for 20–40 min before electrorotation measurements. Conductivity

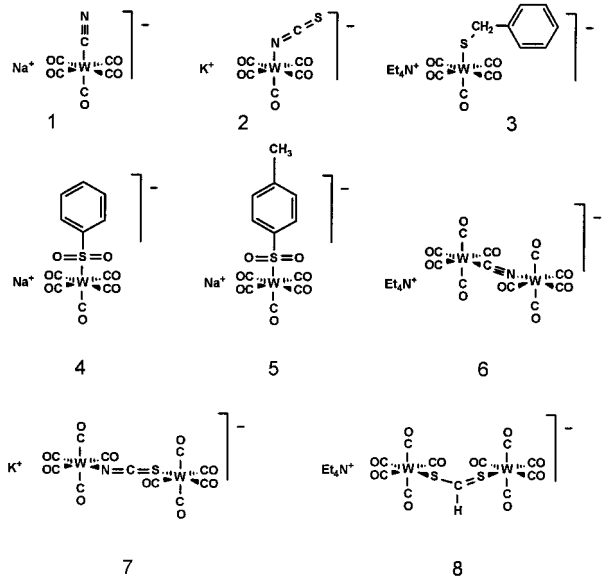

FIGURE 1 Structures of the tungsten carbonyl salts tested here (no., formula, chemical name, formula weight of the anion): (*1*) $Na[W(CO)_5(CN)] \cdot 3H_2O$, sodium pentacarbonylcyanotungstate, 350. (*2*) $K[W(CO)_5(NCS)]$, potassium pentacarbonylthiocyanatotungstate, 382. (*3*) $Et_4N[W(CO)_5(SCH_2C_6H_5)]$, tetraethylammonium pentacarbonylbenzylthiolatotungstate, 447. (*4*) $Na[W(CO)_5(SO_2C_6H_5)]$, sodium pentacarbonylphenylsulfinatotungstate, 467. (*5*) $Na[W(CO)_5(SO_2C_6H_4CH_3)]$, sodium pentacarbonyl-(4-methylphenyl)sulfinatotungstate, 479. (*6*) $Et_4N[W_2(CO)_{10}(\mu\text{-CN})]$, tetraethylammonium decacarbonyl-μ-cyano-ditungstate, 674. (*7*) $K[W_2(CO)_{10}(\mu\text{-SCN})]$, potassium decacarbonyl-μ-thiocyanato-ditungstate, 706. (*8*) $Et_4N[W_2(CO)_{10}(\mu\text{-}S_2CH)]$, tetraethylammonium decacarbonyl-μ-dithioformiato-ditungstate, 725.

and osmolality of the solutions were measured by means of a digital conductometer (Knick GmbH, Berlin, Germany) and a cryoscopic osmometer (Osmomat 030; Gonotec GmbH, Berlin, Germany), respectively, at a temperature of 20–22°C.

The viability of Sp2 cells in the presence of tungsten carbonyl salts was assessed by a colorimetric assay system using 2,3-bis(2-methoxy-4-nitro-5-sulfophenyl)-5-(phenylamino-carbonyl)2H-tetrazolium hydroxide (XTT) (Sigma) and phenanzine methosulfate (PMS) (Serva, Heidelberg, Germany) as described elsewhere (Gröhn et al., 1994). The method (XTT test) is based on the observation that living cells can convert the membrane-permeable, yellow, tetrazolium salt XTT into a water-soluble orange product (Scudiero et al., 1988). The cell proliferation rate was measured by counting cell cultures at 6, 12, 24, 36, 48, . . . , 180 h after the addition of the tungsten compounds.

Rotation chambers and external fields

Two different electrorotation chambers were used in this study. First we used the macroscopic four-electrode chamber that has been described in detail previously (Arnold and Zimmermann, 1988). The rotation of the cells was observed with an inverted microscope (Leica Fluolux). The spacing of the planar electrodes (mounted at right angles to each other) was ~1.2 mm. About 10 μl of the suspension (containing, on average, 10^3 cells) was added to this chamber. Two opposite electrodes were connected to a conductometer to allow the solution conductivity to be monitored. The measurements of the field frequency inducing the fastest antifield rotation (f_{c1}; see Rotation Theory) were performed in the macroscopic chamber by the contrarotating field technique (Arnold and Zimmermann, 1988; Fuhr et al., 1996), which permits accurate and rapid determination of the maximum rotation frequency f_{c1}.

We also used a microstructure chamber developed by G. Fuhr (Humboldt University, Berlin; see Fuhr et al., 1996). Four circular microelectrodes (200-μm diameter) are manufactured on quartz glass (Pyrex 7740) by electroplating gold to the surface to a thickness of 0.95 μm. The distance between two opposing electrode tips was 300 μm. Fifty to seventy microliters of cell suspension was added to electrodes in the chamber and covered with a microslide. The cells in the chamber were observed with a Leica Metallux microscope with long-distance objectives. The microscope was equipped with an LCD video camera connected to a videotape recorder. The electrodes of the microstructure chamber were connected to four 90° phase-shifted, symmetrical square wave signals provided by a computer-controlled pulse generator with an output voltage of 3 V_{PP} (HP8130A; Hewlett Packard, Bad Homburg, Germany). Cell rotation speed was measured with a stopwatch between 100 Hz and 150 MHz at 5–10 points per frequency decade. Only single cells near the center of the chamber were measured. Cell radii were determined with a calibrated ocular micrometer. The rotation spectra were fitted by model 1, 2, or 3 (see below) with *Mathematica* software (Wolfram, 1996).

RESULTS

Synthesis of tungsten carbonyl anions and their cytotoxicity

The tungsten carbonyl anions (Fig. 1) used in this study (see below) were synthesized by established procedures or suitable adaptations thereof. The compounds $Na[W(CO)_5(CN)]$ (**1**) (King, 1967) and $K[W(CO)_5(NCS)]$ (**2**) were prepared by irradiating $[W(CO)_6]$ in tetrahydrofuran (THF) to produce a solution of $[W(CO)_5THF]$ (Strohmeier and Gerlach, 1961), and adding a stoichiometric amount of NaCN or KSCN, respectively. The thiolate complex $Et_4N[W(CO)_5(SCH_2C_6H_5)]$ (**3**) was obtained by reacting $Et_4N[W(CO)_5X]$ (X = Cl, Br) with $NaSCH_2C_6H_5$ in THF. The salts $Na[W(CO)_5(SO_2C_6H_5)]$ (**4**) and $Na[W(CO)_5(SO_2C_6H_4CH_3)]$ (**5**) were synthesized by irradiating $[W(CO)_6]$ and an equimolar amount of the required sodium sulfinate in ethanol. The pseudohalide-bridged binuclear complexes $Et_4N[W_2(CO)_{10}(\mu\text{-CN})]$ (**6**) and $Et_4N[W_2(CO)_{10}(\mu\text{-SCN})]$ (**7**) were assembled from the mononuclear precursors $Et_4N[W(CO)_5(CN)]$ and $Et_4N[W(CO)_5(NCS)]$ (Buchner and Schenk, 1984) and a stoichiometric amount of $[W(CO)_5THF]$. The dithioformate complex $Et_4N[W_2(CO)_{10}(\mu\text{-}S_2CH)]$ (**8**) was finally synthesized by irradiating $[W(CO)_6]$ in ethanol and adding $KHCS_2$ and Et_4NBr. The compounds were purified by crystallization from THF/ether (with a trace of water added for **1**) and characterized by elemental analyses, IR and ^{13}C-NMR (the full details will be described elsewhere). Unlike the usually prepared salts containing large organic cations (Ruff, 1969; Buchner and Schenk, 1984), the alkali salts described here are reasonably soluble in water. The stability of the aqueous solutions was checked by UV/VIS and IR spectroscopy. Compounds **2**, **3**, and **7** slowly decomposed over several days, whereas the others seemed to be infinitely stable in water.

The toxicity of the tungsten carbonyl compounds was assessed by cell proliferation and the XTT test. It was found to be fairly low. At concentrations of up to 10 μM, compounds **1**, **2**, **5**, and **7** did not markedly inhibit growth of the myeloma cells. Compound **8** was somewhat more toxic: 10 μM of this salt significantly reduced the rate of growth in the log phase (to ~20% of the rate in control cell cultures), and 50 μM completely inhibited the proliferation of myeloma cells. The colorimetric viability test (XTT based) gave comparable data on the cytotoxicity of the tungsten compounds. Thus at concentrations of up to 10 μM, salts **1**, **2**, and **6** did not affect the viability of cells for incubation periods as long as 6–7 h. The addition of compounds **1**, **2**, and **6** at a concentration of 50 μM reduced cell viability to 4%, 71%, and 32% of the control level, respectively. The order of the toxicity of these three salts agreed well with their partition coefficients (parameter β), but not with their translocation rate constants (k_i), as obtained by electrorotation experiments (see below).

Electrorotation of cells

Dependence of the antifield peak frequency (f_{c1}) on medium conductivity

The electrical parameters of the plasma membrane (C_m and G_m) can be calculated from the dependence of the antifield peak frequency (f_{c1}) on the conductivity of the aqueous phase. The antifield peak frequency (f_{c1}) was measured by the contrarotating field technique (Arnold and Zimmermann, 1988). The plot of f_{c1} (normalized to the radii of the cells) versus the external conductivity is shown in Fig. 2. The fit of the data obtained from control Sp2 cells (*circles*) at the conductivities below 5 mS m^{-1} (50 partly overlapping symbols represent more than 10^3 cells with the mean radius 8.8 ± 0.9 μm) with Eq. 6 (*solid curve*) yielded the

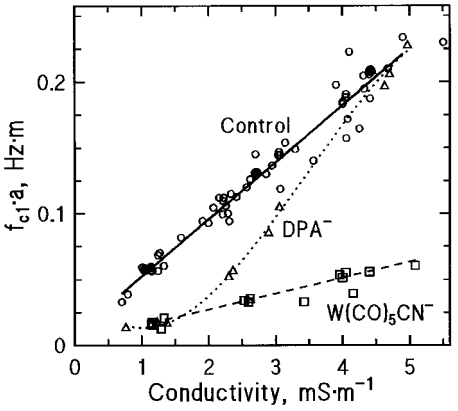

FIGURE 2 Cumulative plot of the characteristic antifield frequencies (f_{c1}) normalized to the cell radius (a) versus the external conductivity (σ_e). The data were obtained by the contrarotating field method (*open symbols*) or from rotation spectra (*filled symbols*). Measurements were performed in hypotonic medium (150 mOsm inositol) on untreated Sp2 cells (*circles*, $a = 8.8 \pm 0.9$ μm, mean $\pm$ SD, $n = 1500$ cells), on Sp2 cells treated with 10 μM DPA^- (*triangles*, $a = 8.6 \pm 0.9$ μm, $n = 180$), and on Sp2 cells treated with 10 μM $[W(CO)_5(CN)]^-$ (*squares*, $a = 8.7 \pm 1.0$ μm, $n = 330$). Each open symbol represents the mean (f_{c1}·a) from 20–40 cells measured at closely similar conductivities; each filled symbol is the mean from 5–10 rotation spectra. For control cells and cells treated with $[W(CO)_5(CN)]^-$, the data obtained at conductivity lower than 5 mS m^{-1} were fitted by Eq. 6 (*solid* and *dashed lines*, respectively). The apparent area-specific membrane parameters ($\pm$ SE of the fits) were found to be, for control cells, $C_m = 7.4 \pm 0.2$ mF m^{-2} and $G_m = 48 \pm 23$ S m^{-2}; for $[W(CO)_5(CN)]^-$-treated cells, $C_m = 26.5 \pm 1.0$ mF m^{-2} and $G_m = 66 \pm 29$ S m^{-2}.

following values: $C_m = 7.4 \pm 0.2$ mF m^{-2} and $G_m = 48 \pm 23$ mS m^{-2}. The values for membrane capacitance and conductance were in good agreement with results that had been derived earlier from Sp2 cells (Sukhorukov et al., 1993, 1994) and those obtained from electrorotation spectra (see below).

Effects of lipophilic anions on the low-frequency antifield peak (f_{c1})

Fig. 2 also shows experimental data obtained with the contrarotating field method from Sp2 cells in the presence of 10 μM DPA^- (*triangles*) and 10 μM $[W(CO)_5(CN)]^-$ (*squares*). Similar to the conditions that have been observed with human erythrocytes (Sukhorukov and Zimmermann, 1996), DPA-treated Sp2 cells showed an upwardly curved dependence of the radius-normalized f_{c1} frequency on the external conductivity (Fig. 2, *triangles* and *dotted line*). At a conductivity of 1.1 mS m^{-1}, the addition of 10 μM DPA^- resulted in a pronounced decrease in the antifield rotation maximum from ~7 kHz (untreated cells) to 1.6 kHz. This corresponded to a fourfold increase in the apparent specific membrane capacity from 6 to 24 mF m^{-2} (the estimate was made by neglecting G_m in Eq. 6 for the mean radius of 9 μm). The increase in medium conductivity from 1.4 to 4.4 mS m^{-1} led to a rapid increase in f_{c1} values from 2 to 23 kHz, i.e., to a decrease in the apparent C_m. At higher conductivities, the f_{c1} a values of DPA-treated cells were close to those obtained from control Sp2 cells.

In contrast to DPA^--treated cells, the conductivity dependence of the f_{c1} a values for Sp2 cells treated with 10 μM $[W(CO)_5(CN)]^-$ was found to be highly linear over a relatively wide range of external conductivity ($\sigma_e < 30$ mS m^{-1}; Fig. 2, *squares*). The least-square fit of Eq. 6 to the data obtained at a σ_e of less than 5 mS m^{-1} (*dashed line*) yields the apparent values for $C_m = 26.5$ mF m^{-2}. Under low-conductivity conditions, qualitatively similar alterations to the antifield rotation peak and to the C_m values of Sp2 cells were induced by tungsten carbonyl anions **2**, **3**, **6–8** (data not shown), whereas carbonyl anions **4** and **5** (10–100 μM) did not cause any change in the position of the antifield plasma-membrane peak. The large capacity values measured here with DPA^- and tungsten carbonyl salts can be viewed as capacity increments, ΔC_m, above that of the unmodified cell membrane obtained by the "null-frequency" technique. These data allow the evaluation of the surface density, N_t, of the adsorbed anions (mobile charges) in the plasma membrane using the equation $N_t = 2\Delta C_m RT/F^2$. This means that a concentration of DPA^- and $[W(CO)_5(CN)]^-$ of 10 μM produced an apparent capacity increase of ~18 and 19 mF m^{-2}, which corresponded to a total surface concentration, N_t, of 9.5 and 10 nmol m^{-2} of adsorbed lipophilic ions, respectively.

It is noteworthy that none of the chemicals used for preparation of the tungsten carbonyl salts was able to increase the apparent specific capacitance of the plasma membrane. The C_m values (obtained by means of the "null-frequency" technique; see above) of Sp2 cells treated with 10–100 μM $[W(CO)_6]$, $[W(CO)_5THF]$, KSCN, and NaCN, and 20–50 μM Et_4NCl and Et_4NBr (data not shown) did not differ significantly from that of control cells.

Rotation spectra of control cells

Electrorotation spectra of control Sp2 cells at different external conductivities ranging from 10 to 230 mS m^{-1} are shown in Fig. 3 (*open symbols*). In these experiments we used low-osmolality media (150 mOsm) because hypotonic cell swelling significantly reduced variations in the individual C_m values of myeloma cells caused by the disappearance of membrane folds and microvilli (Sukhorukov et al., 1993; Wang et al., 1994a). The increase in external conductivity shifted the major antifield rotation peak to a higher frequency, from 63 kHz at 10 mS m^{-1} to 400 kHz at 230 mS m^{-1}. The fastest antifield rotation of ~9 radian/s was observed at low conductivity, $\sigma_e = 10$ mS m^{-1} (Fig. 3 *A*). With increasing external conductivity, the magnitude of this "plasma membrane" peak decreased gradually to become 2.75 radian/s at 230 mS m^{-1}. An increase in the external conductivity had little effect on the "cytosolic" cofield peak (4–5 radian/s at 25–40 MHz) until ~60 mS m^{-1} was reached. In more conductive media, the cofield peak moved toward higher frequencies ($f_{c2} > 100$ MHz), and its mag-

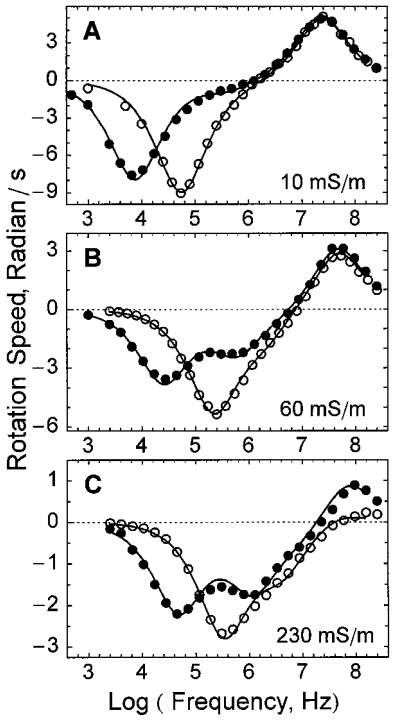

FIGURE 3 Rotation spectra of control cells (*open symbols*) and cells treated with 10 μM $[W(CO)_5(CN)]^-$ (*filled symbols*) measured at different external conductivities: 10 mS m^{-1} (*A*), 60 mS m^{-1} (*B*), and 230 mS m^{-1} (*C*), but at the same osmolality (150 mOsm). The curves are best fits of model 2 (control) and model 3 (treated cells) to the experimental data. (For the cellular and mobile charge parameters derived by curve fitting, see text and Table 1.)

nitude decreased rapidly to $\Omega = 0.25$ radian/s (at 230 mS m^{-1}).

Most rotation spectra of untreated Sp2 cells exhibited an additional, poorly resolved peak or "shoulder" at frequencies of ~1–2 MHz. Therefore, model 1 was not applicable to the analysis of the rotation spectra of Sp2 cells, because this model requires two symmetrical peaks. The deviations from the single-shell model reflect at least one dispersion that may arise from the polarization of the nucleus and from the frequency-dependent dielectric properties of cytosolic macromolecules (see Discussion). The continuous curves in Fig. 3 represent the best-fit theoretical spectra calculated with model 2 (a single-shelled cell exhibiting a dispersion of the cytoplasm) to the experimental data obtained over the whole conductivity range from 3 to ~200 mS m^{-1}. The electrical parameters of the plasma membrane, $C_m = 6.5$ mF m^{-2} and $G_m = 100$–200 S m^{-2}, deduced from the spectra agreed well with the C_m and G_m values obtained by the "null-frequency" technique in low-conductivity solutions (see Fig. 2). For the fit of the rotation spectra of Sp2 cells, the following cytoplasmic parameters were assumed: $\sigma_{il} = 0.13$–0.27 S m^{-1}, $\sigma_{ih} = 0.32$–0.58 S m^{-1}, $\epsilon_{il} = 10^3$-1.5×10^3 ϵ_0, $\epsilon_{ih} = 120$ ϵ_0, $f_{di} = 4.0 \pm 0.7$ MHz. As judged by the correlation coefficients ($\rho > 0.997$), model 2 provided a very good approximation to the data obtained on control myeloma cells. The values of the internal conductivities (σ_{il} and σ_{ih}) decreased gradually with decreasing external conductivity. This was clearly due to ion leakage from the cytoplasm of cells, which were exposed to hypotonic low-salinity electrorotation media for 20–40 min.

Effect of tungsten carbonyl compounds on electrorotation spectra

Rotation spectra of Sp2 cells in media of different conductivities, but with the same concentration of the lipophilic anion $[W(CO)_5(CN)]^-$ (10 μM), are depicted in Fig. 3 (*filled symbols*). The treatment of the cells with $[W(CO)_5(CN)]^-$ resulted in dramatic, conductivity-dependent changes in the antifield rotation, i.e., in the part of the spectrum that is influenced by the electrical properties of the plasma membrane. Under low-conductivity conditions ($\sigma_e = 10$ mS m^{-1}), addition of the anion to the external medium led to a marked decrease in the major antifield rotation maximum to a lower frequency from 56 kHz (control cells, *open circles*) to 8 kHz ($[W(CO)_5(CN)]^-$-treated cells, *filled circles*). With increasing external conductivity, this antifield rotation maximum, which is caused by the adsorption of the mobile charges to the plasma membrane, moved toward higher frequencies. The characteristic frequency of the mobile charges' peak (the f_{c1} value) increased rapidly at first from 8 kHz (10 mS m^{-1}; Fig. 3 *A*, *filled circles*) to 25 kHz (60 mS m^{-1}; Fig. 3 *B*), then more slowly to 45 kHz (144 mS m^{-1}; not shown). The use of media of higher conductivity up to 230 mS m^{-1} (Fig. 3 *C*) caused only a little further change in the position of the mobile charges' peak. The rotation speed of the cells decreased gradually from 8 radian/s at 10 mS m^{-1} to 2.2 radian/s at 230 mS m^{-1}. The f_{c1} values evaluated from rotational spectra, which agreed well with the data obtained by the contrarotating field method, are shown in Fig. 2.

At intermediate conductivity (e.g., 60 mS m^{-1}; Fig. 3 *B*), an additional, well-resolved antifield peak centered at ~1 MHz appeared in the rotation spectra of Sp2 cells treated with $[W(CO)_5(CN)]^-$. The relative magnitude of this peak, which is mainly dominated by the geometrical electrical parameters of the plasma membrane, C_m and G_m, increased gradually with increasing medium conductivity (Fig. 3, *A–C*). Similar to the control Sp2 cells, the "cytosolic" cofield rotation of cells treated with $[W(CO)_5(CN)]^-$ moved toward a higher frequency and became slower as the conductivity of the suspending medium was increased.

The curves of Fig. 3 (*solid symbols*) are the best-fit theoretical spectra obtained with model 3 (the mobile charge model with a dispersion of the cytoplasm). The mobile charge parameters deduced by fitting the data are listed in Table 1 (see also legend to Fig. 3). As with the untreated cells (*open symbols*), the σ_{il} and σ_{ih} values grew with increasing external conductivity. For the fit of the rotation spectra shown in Fig. 3, the following parameters were assumed (mean ± SE): $C_{mh} = 6.87 \pm 0.05$ mF m^{-2}, $G_{ml} = 144 \pm 20$ S m^{-2}, $\sigma_{il} = 0.36 \pm 0.03$ S m^{-1}, $\sigma_{ih} = 0.46 \pm 0.03$ S m^{-1}, $\epsilon_{ih} = 103 \pm 2$ ϵ_0, $f_{idisp} = 6.2 \pm 0.4$

TABLE 1 Parameters of the mobile charges in the plasma membrane of Sp2 cells and in the artificial lipid bilayer formed of DOPC in the presence of different tungsten carbonyl anions and DPA^-

Anion	Membrane	n	c (μM)	N_t (nmol m^{-2})	$\beta = N_t/2c$ (μm)	k_i (10^5 s^{-1})
$[W(CO)_5(CN)]^-$	Cells	4	1	7.6	3.8	4.5
1		4	2	10.5	2.6	3.7
		3	5	19.2	1.9	3.7
		4	10	20.2	1.0	2.0
		3	20	22.1	0.55	1.9
		3	50	28.2	0.28	1.6
$[W(CO)_5(CN)]^-$	Bilayer	10	0.045	0.95	10.5	1.00
1		14	0.135	3.76	14.0	0.98
		15	0.45	32.7	36.3	0.42
		7	1.35	57.8	21.4	0.19
		7	4.5	55.3	6.1	0.12
$[W(CO)_5(NCS)]^-$	Cells	7	5	1.8	0.18	4.7
2		10	10	3.6	0.18	3.9
		12	20	7.4	0.19	4.9
		10	30	7.7	0.13	4.1
		5	50	11.8	0.12	3.7
$[W(CO)_5(NCS)]^-$	Bilayer	7	0.03	0.12	1.96	1.34
2		7	0.1	0.11	0.55	1.40
		10	0.3	0.12	0.20	1.32
		7	1	0.50	0.25	0.99
		10	3	2.51	0.42	0.88
		9	10	14.9	0.75	0.70
		8	30	36.6	0.61	0.43
$[W(CO)_5(SCH_2C_6H_5)]^-$	Cells	7	5	11.8	1.18	0.9
3		7	10	10.0	0.50	1.3
		5	20	12.4	0.31	1.2
		8	50	17.7	0.18	0.7
$[W_2(CO)_{10}(CN)]^-$	Cells	4	0.1	5.7	28.5	4.2
6		4	0.5	19.4	19.4	2.3
		3	1	15.0	7.5	3.1
		3	5	19.6	1.96	2.2
		4	10	15.2	0.76	2.5
		3	20	14.5	0.36	2.7
		3	50	17.2	0.18	2.6
$[W_2(CO)_{10}(S_2CH)]^-$	Cells	4	0.5	5.1	5.1	5.8
8		4	1	17.7	8.9	3.7
		5	2	14.8	3.7	2.8
		5	5	22.3	2.2	1.7
DPA^-	Cells	3	5	21.0	2.1	0.16
		3	10	21.9	1.1	0.12
		3	20	27.8	0.70	0.15
		3	40	34.8	0.44	0.15

n is the number of experiments.

MHz, $N_t = 18.3 \pm 1.1$ nmol m^{-2}, $k_i = (2.6 \pm 0.3)\ 10^5\ s^{-1}$, which had all correlation coefficients higher than 0.991 in the fit procedure. This result demonstrated the usefulness of model 3 for the analysis of the electrorotation spectra of myeloma cells treated with $[W(CO)_5(CN)]^-$ over the wide range of external conductivity used here. For Sp2 cells treated with lipophilic anions **1–3** and **6–8**, the dependence of the rotation peaks on suspension conductivity was qualitatively similar to results obtained from Sp2 cells treated with $[W(CO)_5(CN)]^-$. For DPA-treated Sp2 cells, two well-resolved antifield rotation peaks could be observed at much lower external conductivities (3–6 mS m^{-1}). At higher conductivities (>10 mS m^{-1}), the plasma membrane peak dominated the rotation spectra, whereas the low-frequency, mobile charges' peak due to DPA^- became negligible (data not shown). In contrast to the situation described above, the rotation spectra of cells in the presence of $Na[W(CO)_5(SO_2C_6H_5)]$ (**4**) and $Na[W(CO)_5(SO_2C_6H_4CH_3)]$ (**5**) (10–100 μM) were identical to those measured on control cells. This means that compounds **4** and **5** did not introduce mobile charges (detectable by electrorotation) into the plasma membrane of myeloma cells.

Effect of different concentrations of lipophilic anions on electrorotation spectra

Fig. 4 shows rotation spectra of Sp2 cells after treatment with different concentrations of the tungsten compound $[W_2(CO)_{10}(S_2CH)]^-$ (**8**). Each spectrum represents the

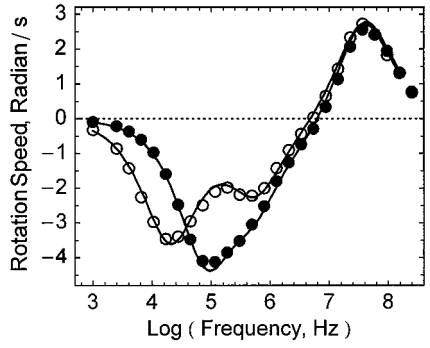

FIGURE 4 Rotation spectra of Sp2 cells in the presence of 0.5 μM (*filled circles*) and 5 μM (*open circles*) $[W_2(CO)_{10}(S_2CH)]^-$ measured at 60 mS m^{-1} (150 mOsm). The mobile charges' parameters extracted by fitting model 3 (*curves*) to the 0.5 (5) μM data are $N_t = 4.1$ nmol m^{-2} and $k_i = 5.8 \times 10^5$ s^{-1} ($N_t = 23$ nmol m^{-2} and $k_i = 1.6 \times 10^5$ s^{-1}).

mean obtained from four or five cells measured at the same external conductivity (~60 mS m^{-1}). The rotation spectrum of untreated cells at 60 mS m^{-1} is depicted in Fig. 3 *B* (*open circles*). In the presence of 0.5 μM $[W_2(CO)_{10}(S_2CH)]^-$ (Fig. 4, *filled circles*), the fastest rotating field-induced antifield rotation was shifted from 250 kHz (control cells) to 100 kHz. Furthermore, a distinctive asymmetry occurred in the antifield part of the spectrum. At this low anion concentration (0.5 μM), the plasma membrane peak and the somewhat overlapping mobile charge peak resulted in a broad antifield rotation maximum. An increase in the lipophilic ion concentration allowed progressively better resolution of the two antifield maxima. This means that in medium containing 5 μM $[W_2(CO)_{10}(S_2CH)]^-$ (Fig. 4, *open circles*), the rotation spectrum exhibited well-resolved peaks at 20 kHz (caused by the adsorbed mobile charges) and 500 kHz (due to the electrical properties of the plasma membrane). The other tungsten carbonyl anions tested in this study (except for **4** and **5**) and DPA^- showed qualitatively similar concentration effects on the rotation spectra of Sp2 cells.

Charge pulse experiments

In all experiments with the negatively charged lipophilic ions adsorbed to lipid bilayers, two exponential relaxations were resolved. Whereas the first (fast) purely exponential relaxation process is coupled with the distribution of lipophilic ions within the membrane and is a function of k_i; the second, slow relaxation process reflects the RC-time constant, τ_m (produced by a resistor in parallel with the electrodes and the membrane capacitance), and the redistribution of lipophilic ions. Accordingly, τ_2 was always considerably larger than τ_m because of the adsorbed lipophilic ions (Benz et al., 1976). From the parameters of the two relaxation processes, the translocation rate constant, k_i, the total surface concentration, N_t, and τ_m were calculated according to Eqs. 1–3, using the specific capacitance of DOPC/*n*-decane membranes ($C_m = 3.7$ mF m^{-2}; Pickar and Benz, 1978).

For each set of experimental conditions, at least six membranes were used. The standard deviations were usually less than 20% for k_i and less than 35% for N_t. The larger variations for N_t are presumably caused by the difficulty in obtaining partition equilibrium, which is caused by the high partition coefficient of the lipophilic ions. Because the fit of the experimental data was always very accurate, the deviations mentioned above for the parameters k_i and N_t represented the variations in the individual membranes.

Fig. 5 (*open symbols*) and Table 1 show the experimental data (N_t, k_i, and β) of the charge pulse experiments performed with the different tungsten carbonyl anions on the artificial bilayer membranes made of DOPC. The maximal translocation rate constant of $[W(CO)_5(NCS)]^-$ ($k_i = 1.4 \times 10^5$ s^{-1}) was somewhat higher than the k_i of $[W(CO)_5(CN)]^-$ (1.05×10^5 s^{-1}). For both anions, the translocation rate decreased gradually with increased concentration of mobile charges in the membrane. Replacement of the cyanide residue (**1**) by a rhodanide one (**2**) yielded a marked difference in the partitioning behavior of the metal carbonyl anions. Thus the partition coefficient measured for $[W(CO)_5(CN)]^-$ ($\beta = 36$ μm, $c = 0.45$ μM) was higher by at least two orders of magnitude than β of $[W(CO)_5(NCS)]^-$ ($\beta = 0.2$–0.33 μm, $c = 0.3$–1 μM), indicating much higher lipophilicity of the cyanide complex as compared with the rhodanide one.

DISCUSSION

Influence of the cell structure on the rotation spectra of control cells

The study of Sp2 cell structure by phase-contrast and transmission electron microscopy (data not shown) demonstrated

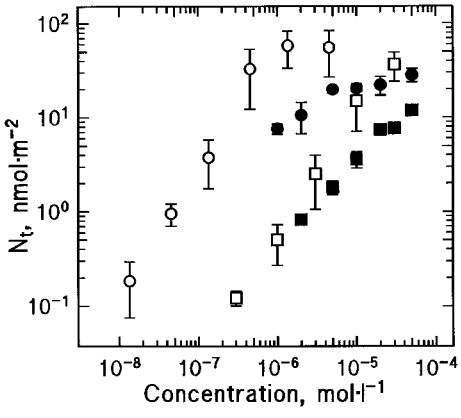

FIGURE 5 The area-specific concentration of the mobile charges (N_t) within the plasma membrane of Sp2 cells (*filled symbols*) and in the lipid bilayers formed from DOPC (*open symbols*) as a function of the bulk anion concentration: $[W(CO)_5(CN)]^-$ (*circles*) and $[W(CO)_5(NCS)]^-$ (*squares*). The data were derived from electrorotation (*filled symbols*) and charge pulse relaxation studies (*open symbols*).

that these cells contain cell organelles and a relatively large nucleus surrounded by two membranes. Under the hypoosmotic conditions (150 mOsm) used in our electrorotation measurements, most Sp2 cells had the shape of spheres and contained an almost spherical nucleus that was separated from the plasma membrane by a thin, uniform cytoplasmic layer. The morphological analysis of representative cells ($n = 25$) gave mean values ($\pm$ SD) for the radii of the cell and nucleus of $a_c = 9.2 \pm 0.7$ μm and $a_n = 6.7 \pm 0.8$ μm, respectively. Because of the large size of the nucleus, the Sp2 cells should create a marked "Maxwell-Wagner" dispersion with the interrelated dispersion increment $(\epsilon_{il} - \epsilon_{ih}) = \tau_d \cdot (\sigma_{ih} - \sigma_{il})$. The expected values of f_d and $\Delta\epsilon_i = (\epsilon_{il} - \epsilon_{ih})$ or $\Delta\sigma_i = (\sigma_{ih} - \sigma_{il})$ for a typical Sp2 cell can be calculated using the first-order approximations given by Schwan (1988): $\Delta\epsilon_i = a_n C_n \sigma_i^2/(\sigma_i + a_n G_n)^2$ and $f_d = (\sigma_i + a_n G_n)/(2\pi a_n G_n)$. When we take into account the double-membrane structure of the nuclear envelope (two closely spaced lipid membranes in series), the effective nuclear specific capacity C_n would be $\sim$4 mF m^{-2}, which is half of the typical C_m value for a single biological membrane (7–8 mF m^{-2}). Assuming an internal conductivity $\sigma_i = 0.5$ S m^{-1} and a nuclear radius $a_n = 6.7$ μm (see above), and neglecting the product radius times conductivity of the nuclear envelope ($a_n G_n$), a dispersion of the cytosol with the increment $\Delta\epsilon_i = 3000\ \epsilon_0$ can be expected to occur at $\sim$3 MHz rotational frequency. Electrorotation measurements of control Sp2 cells (Fig. 3) seem to confirm our assumption that the internal dispersion of Sp2 cells was mainly due to the polarization of their large nucleus. Other dispersion mechanisms, such as polarization of the intracellular macromolecules and the small-sized organelles, did not influence the electrorotational behavior of Sp2 cells significantly, at least within the conductivity range of 1–200 mS m^{-1} considered here.

Adsorption of tungsten carbonyl anions to the cell membrane

From the electrorotational spectra of the individual cells (similar to those shown in Figs. 3 and 4), the total specific surface concentration (N_t) and the translocation rate constant (k_i) of the lipophilic anions within the plasma membrane could be derived by using the mobile charge model (model 3) to fit the experimental data. To compare the adsorption of the different tungsten carbonyl anions (**1–8**) to those of DPA^-, measurements were performed in which the external concentrations of the anions were varied over a wide range from 0.1 to 50 μM. The values of k_i and N_t deduced for different lipophilic anions adsorbed to the plasma membrane of Sp2 cells are summarized in Table 1. The concentration N_t of the mobile charges in the plasma membrane of the Sp2 cells increased with increasing concentration of the lipophilic anions (see Table 1 and Fig. 5, *filled symbols*). However, the adsorption of the tungsten compounds varied considerably for different compounds. In the case of $[W(CO)_5(CN)]^-$, the addition of the anion at a concentration of 1 μM (or higher) resulted in an easily detectable concentration of mobile charges adsorbed to the plasma membrane ($N_t > 2$ nmol m^{-2}). In contrast, a much higher concentration of $[W(CO)_5(NCS)]^-$ ($c > 5$ μM) had to be added to the external media to induce a detectable concentration of mobile charges in the plasma membrane of Sp2 cells. For most tungsten compounds used here, the total surface concentration, N_t, increased, and the partition coefficient, $\beta = N_t/2c$, decreased gradually with increasing concentration of the anions in the aqueous phase. The decrease in β is probably caused by the generation of boundary potentials (Benz et al., 1976; Wulf et al., 1977). Comparison of the partition coefficients of the different anions at a concentration of 5 μM demonstrated that their lipophilicity decreased in the order $[W_2(CO)_{10}(S_2CH)]^- > DPA^- > [W_2(CO)_{10}(CN)]^- > [W(CO)_5(CN)]^- \gg [W(CO)_5(SCH_2C_6H_5)]^- \gg [W(CO)_5(NCS)]^-$. It is noteworthy that the results of Fig. 5 revealed a remarkable difference in the partition coefficients of two anions, the structures of which are similar in terms of molecular mass, size, and shape: $[W(CO)_5(CN)]^-$ ($\beta_1 = 1.9$ μm at $c = 5$ μM) and $[W(CO)_5(NCS)]^-$ ($\beta_2 = 0.18$ μm at $c = 5$ μM). These data agree with the results obtained from artificial lipid membranes with the charge pulse relaxation technique (see below).

Rate constants of tungsten carbonyl anion transport through cell membranes

Table 1 also contains the translocation rate constants (k_i) of the different tungsten compounds through the plasma membrane of the Sp2 cells. There was a considerable difference in the absolute values of the translocation rates for different anions and membranes. The highest k_i was measured for $[W_2(CO)_{10}(S_2CH)]^-$ ($k_i = 5.8 \times 10^5$ s^{-1}), whereas the lowest k_i values were found for the two lipophilic anions that contained aromatic moieties $[W(CO)_5(SCH_2C_6H_5)]^-$ ($k_i = 0.7 \times 10^5$ s^{-1}) and DPA^- ($k_i = 0.13 \times 10^5$ s^{-1}, two aromatic rings). Comparison of the translocation rate constants k_i for the lipophilic anions demonstrates that their mobility within the plasma membrane decreases in the following order: $[W_2(CO)_{10}(S_2CH)]^- > [W(CO)_5(NCS)]^- > [W(CO)_5(CN)]^- > [W_2(CO)_{10}(CN)]^- \gg [W(CO)_5(SCH_2C_6H_5)]^- \gg DPA^-$. With some other compounds, no dispersion was observed in the rotational spectra: $[W(CO)_5(SO_2C_6H_5)]^-$, $[W(CO)_5(SO_2C_6H_4CH_3)]^-$, $TPhB^-$, and $TPhP^+$. The lack of mobile charges in the plasma membranes of cells treated with these compounds containing aromatic rings may be caused by their poor adsorption to the membrane and/or by their extremely slow translocation rate constants k_i (Pickar and Benz, 1978; Flewelling and Hubbell, 1986). The data of Table 1 demonstrate that the saturation of membrane adsorption of anions **1**, **6**, and **8** was accompanied by a gradual decrease in their translocation rate constants k_i, whereas the k_i values of compounds **2**, **3**, and DPA^- remained nearly unchanged. This may again

be caused by the generation of boundary potentials, which tend to decrease both the adsorption and transport kinetics of lipophilic ions (Andersen et al., 1978). The results presented in Table 1 indicate that the influence of the structural changes, such as the molecular size or mass, on the translocation rate constants of compounds **1**, **2**, **6**, and **8** was very small. In contrast, the translocation and partition coefficients of the derivatives of $W(CO)_5$ were strongly affected by the attachment of an aromatic ring (anions **3–5**). It is noteworthy that the values deduced for the translocation rate of DPA^- in the plasma membrane of Sp2 cells were in good agreement with those published in the literature for DPA-treated nerve cells (12×10^3 s^{-1}; Benz et al., 1984), for DPA^--treated human erythrocytes (30×10^3 s^{-1}; Sukhorukov and Zimmermann, 1996), and for solvent-free, DPA^--doped planar lipid bilayer membranes (30×10^3 s^{-1}; Dilger and Benz, 1985). Evidently, most tungsten carbonyl anions translocate across the plasma membrane much faster (at least by one order of magnitude) than DPA^- anions. An increase in the translocation rate shifts the membrane dispersion toward higher frequency (see Eq. 8).

Comparison of the lipid bilayer and cell membrane data

It is noteworthy that the data derived here from electrorotation experiments are in good agreement with those that have been obtained previously by the charge pulse technique. This means that DPA^- showed a translocation rate that was 40 times higher and a somewhat higher partition coefficient in biological and artificial membranes as compared to $TPhB^-$ (Benz et al., 1976, 1984; Benz and Conti, 1981). The results presented in Table 1 (see also Fig. 5) indicate that the tungsten carbonyl anions (**1** and **2**) show a much smaller partition into the plasma membrane as compared to that in artificial lipid bilayer membranes. This difference between biological and artificial membranes agrees with earlier studies with DPA^- adsorbed to the axolemma of frog nerve and to membranes formed from egg phosphatidylcholine (Benz and Nonner, 1981). The partition coefficients of some amphipathic compounds (e.g., chlorpromazine) were also found to be smaller (by a factor of 1.2–3) in cell membranes than in lipid vesicle membranes (Luxnat et al., 1984). The possible reasons for exclusion of the tungsten carbonyl anions from the plasma membrane of Sp2 cells may be a large area of the membrane proteins, as well as the negative surface potential of the plasma membrane due to negative charges of the lipids or membrane proteins.

From the charge-pulse relaxation experiments on lipid planar bilayer membranes in the presence of the three tungsten carbonyl anions **1**, **2**, and **7**, the concentration per unit membrane area, N_t, and the translocation rate constants, k_i, could be evaluated using Eqs. 1–3 (Table 1, data for compound **7** not shown). Calculations of the partition coefficient ($\beta = N_t/2c$) at a given c show that β decreases in the following order: $[W(CO)_5(CN)]^- \gg [W_2(CO)_{10}(NCS)]^- \gg [W(CO)_5(NCS)]^-$. There exists a good correlation between β of these anions measured in artificial and cell membranes (Fig. 5) and their ability to increase the low-frequency capacitance of the plasma membrane, C_{ml}, as revealed in an earlier study on Sp2 cells (Nielsen et al., 1996). Comparison of the highest k_i values obtained here and reported in the literature shows that the mobilities of the various lipophilic anions in artificial bilayers were in the order $[W(CO)_5(NCS)]^- > [W_2(CO)_{10}(NCS)]^- > [W(CO)_5(CN)]^- \gg DPA^-$. This order is in fair agreement with that of the translocation rate constants in the cell membrane (see above). The values of k_i for anions **1** ($1.6–4.5 \times 10^5$ s^{-1}) and **2** ($3.7–4.9 \times 10^5$ s^{-1}) dissolved in the plasma membrane are clearly at the upper end of the range measured in bilayer experiments (10^5 and 1.4×10^5 s^{-1} for **1** and **2**, respectively). A similar effect has also been observed for the transport of DPA^- in artificial and biological membranes, which is caused by the thickness of solvent-containing and solvent-free membranes (Benz and Nonner, 1981; Dilger and Benz, 1985).

Applications of lipophilic ions

As mentioned above, lipophilic ions represent an important tool for the study of the structure of biological and artificial membranes, such as thickness, viscosity, surface, and dipole potentials. Unlike most other ions and charged molecules, lipophilic ions readily permeate biological membranes and introduce substantial intrinsic charges and potentials within the membrane, which can strongly influence both carrier-mediated and unassisted ion transport across membranes (Klodos et al., 1995; Bühler et al., 1991). It was shown that an increased charge density caused by the adsorption of lipophilic anions modifies ζ-potential and the electrophoretic mobility of cells and liposomes exposed to DC electric fields (Smejtek and Wang, 1991). The ability of DPA^- to increase the electrical polarizability of membranes is also widely used in high-resolution measurements of the tight junction, membrane fusion, and secretory response of cells, using the capacitance recording in patch-clamped cells (Turin et al., 1991; Oberhauser and Fernandez, 1995). The use of lipophilic ions with faster rates of translocation, such as $[W(CO)_5(CN)]^-$, etc., studied here, will improve the resolution of cell capacitance measurements (Oberhauser and Fernandez, 1995). Furthermore, treatment with lipophilic ions will not only modify the electrorotation spectra of cells (see Figs. 4 and 5), but will also strongly affect the induced membrane voltage (V_m) and the dielectrophoretic (DEP) spectra of cells exposed to AC electric field for electromanipulation (Fig. 6). Therefore, lipophilic ions may be of interest for biotechnology, in which AC and pulsed electric fields are widely used for electrofusion, electropermeabilization, trapping, and separation of cells (Becker et al., 1995; Sukhorukov et al., 1995; Schnelle et al., 1996; Lynch and Davey, 1996; Zimmermann and Neil, 1996).

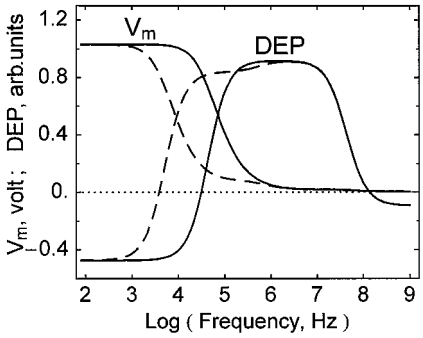

FIGURE 6 Frequency dependence of the dielectrophoretic force (DEP) and of the induced membrane voltage (V_m) in control cells (*solid lines*) and in cells treated with lipophilic anions (*dashed lines*) suspended in a medium of conductivity $\sigma_e = 0.01$ S m^{-1} ($\epsilon_e = 80$). The dielectrophoretic force is given by the real part of the complex cell polarizability (Eq. 4). The theoretical curves for control cells were calculated on the basis of model 1, using the following cellular parameters: $a = 7$ μm, $C_m = 10$ mF m^{-2}, $G_m = 50$ S m^{-2}, $\sigma_i = 0.5$ S m^{-1}, $\epsilon_e = 60$. The curves for treated cells were calculated on the basis of model 3 (mobile charges). The cellular and mobile charge parameters were assumed to be $a = 7$ μm, $C_{mh} = 10$ mF m^{-2}, $G_{ml} = 50$ S m^{-2}, $\sigma_i = 0.5$ S m^{-1}, $\epsilon_e = 60$, $k_i = 2 \times 10^5$ s^{-1}, $N_t = 37.5$ nmol m^{-2}. The dielectrophoretic crossover frequency, f_{d1}, roughly corresponds to the characteristic rotation frequency f_{c1}. Note that mobile charges shift f_{d1} toward lower frequencies.

CONCLUSIONS

Electrorotation measurements performed over a wide range of medium conductivity enabled a detailed analysis of the kinetics of the transport of lipophilic ions in the plasma membrane of cells, using the dielectric single-shell model extended to the case of the membrane containing mobile charges. For cells treated with lipophilic anions, electrorotation allowed the evaluation not only of the passive electric properties in terms of conductivity and permittivity of the plasma membrane and cytoplasm, but also of the surface concentrations and translocation rate constants of the lipophilic anions adsorbed to the plasma membrane. Because of their relatively low toxicity, the lipophilic tungsten carbonyl anions proved to be useful field-sensitive probe molecules for membrane structure and ion transport studies on living cells. Electrorotation of cells treated with tungsten carbonyl anions also provides a tool for analysis of changes in the membrane properties upon exposure of cells to drugs, toxins, electromagnetic radiation, etc.

APPENDIX: THEORETICAL CONSIDERATIONS

Transport of lipophilic ions across lipid membrane

The theory of the movement of lipophilic ions across lipid bilayers and biological membranes was given in full detail in previous publications (Ketterer et al., 1971; Benz et al., 1976; Läuger et al., 1981). Here we will only summarize the basic assumptions and list the equations that allow the calculation of the transport parameters from the experimental results. It is assumed that the lipophilic ions are adsorbed to both sides of the membrane with a total concentration of N_t per unit surface (partition coefficient $\beta = N_t/2c$, where c is the concentration of the lipophilic ions in the aqueous phase). It is assumed that at zero membrane potential, the lipophilic ions are equally distributed between the two membrane-solution interfaces and cross the intermediate free energy barrier with the same rate constant, k_i, in either direction. Under these conditions, the shape of the barrier has no influence on the characteristics of the voltage relaxations measured in a charge pulse experiment, as long as the initial membrane potential is much smaller than 25 mV (Benz et al., 1976; Benz and Conti, 1981). We neglect the exchange of lipophilic ions between the membrane and the aqueous phase during a single relaxation experiment, because it is rate limited by slow aqueous diffusion (Benz et al., 1976).

Charge pulse technique

In a charge pulse experiment, the system is in equilibrium at times $t < 0$, and the membrane capacitance is charged instantaneously at $t = 0$ to an initial voltage V_0 (< 25 mV). The decay of the membrane voltage with time, $V(t)$, is given by the sum of two exponential relaxations:

$$V(t) = V_0(a_1 e^{-t/\tau_1} + a_2 e^{-t/\tau_2}) \tag{1}$$

where a_1, a_2 ($= 1 - a_1$), τ_1, and $\tau_2 > \tau_1$ are known functions of k_i, N_t, and τ_m (Benz et al., 1976; Läuger et al., 1981). The inverse relations between the relaxation parameters and k_i, N_t, and τ_m are given by

$$k_i = \frac{1}{2}\left(\frac{a_1}{\tau_2} + \frac{a_2}{\tau_1}\right) \tag{2}$$

$$N_t = \frac{2RTC_m}{F^2 k_i}\left(\frac{1}{\tau_1} + \frac{1}{\tau_2} - 2k_i - \frac{1}{\tau_m}\right) \tag{3}$$

where $\tau_m = 2k_i\tau_1\tau_2$; C_m is the specific capacitance of the membrane [F m^{-2}]; and R, T and F have their usual meanings.

Rotation theory

The electrorotation spectra of biological cells and other microscopic particles are related to their effective polarizability (f_{CM}) as follows (Arnold and Zimmermann, 1988; Fuhr et al., 1996; Gascoyne et al., 1995; Jones, 1995; Pastushenko et al., 1985; Schwan, 1988):

$$\Omega = -\frac{\epsilon_e E^2 \,\mathrm{Im}(f_{CM})}{2\eta} \tag{4}$$

where Ω is the frequency-dependent rotation speed; ϵ_e and η are the real absolute permittivity and the dynamic viscosity of the medium, respectively; E is the strength of the rotating field; and Im(f_{CM}) is the imaginary part of the Clausius-Mosotti factor, f_{CM}. The factor f_{CM} represents the frequency-dependent polarizability of the cell with respect to the medium. For spherical particles, the polarizability factor is given by (Arnold and Zimmermann, 1988; Fuhr et al., 1996; Gascoyne et al., 1995; Jones, 1995) $f_{CM} = (\epsilon_p^* - \epsilon_e^*)/(\epsilon_p^* + 2\epsilon_e^*)$. The complex permittivity of particles (subscript p) and external media (subscript e) with frequency-independent parameters ϵ (real permittivity) and σ (real conductivity) are defined as $\epsilon^* = \epsilon - j\sigma/\omega$, where ϵ and σ are given in [F m^{-1}] and [S m^{-1}], respectively; $j = (-1)^{1/2}$; and $\omega = 2\pi f$ is the radian field frequency.

Rotation spectra of a biological cell consist of a set of (at least two) co- and antifield rotation maxima. These complex spectra can be explained by modeling cells as single- or multiple-layered spheres, as shown below for three different cases:

1. The electrical properties of cellular compartments (plasma membrane, cytoplasm, nucleus, etc.) can be assumed to be frequency-independent (nondispersive model) (Fuhr et al., 1996; Hölzel, 1997).

2. Additional maxima or shoulders in the rotation spectra of cells arise when the electrical properties of cellular components are frequency-dependent (dispersive).

3. Dispersions of the plasma membrane may be induced by the adsorption of lipophilic ions (Sukhorukov and Zimmermann, 1996) and by mobile charges associated with ion transport systems (Wang et al., 1997b). The simplest single-shell model (model 1) matched well the rotation spectra of control Sp2 cells in low-conductivity solutions ($\sigma_e < 10$ mS m^{-1}). However, for higher medium conductivity and for cells treated with lipophilic anions, more complicated dispersive models had to be introduced (models 2 and 3).

Single-shell nondispersive model (model 1)

In the single-shell model, a cell is approximated by a homogeneous, conductive sphere of radius a, surrounded by a low conducting shell of thickness d, corresponding to the membrane. Taking into account that $d \ll a$, a simplified expression for the complex permittivity of such a particle (Eq. 5) can be derived from the original equation of Pauly and Schwan (1959):

$$\epsilon_p^* = \frac{C_m^* a \cdot \epsilon_i^*}{C_m^* a + \epsilon_i^*} \tag{5}$$

where ϵ_i^* is the complex permittivity of the cytosol, and C_m^* is the complex membrane capacitance per unit area, given by $C_m^* = C_m - j\,G_m/\omega$, where $C_m = \epsilon_m/d$ and $G_m = \sigma_m/d$ are the specific membrane capacitance [F m^{-2}] and conductance [S m^{-2}], respectively. For a single-shelled particle, the theoretical dependence of Ω on field frequency, i.e., the rotation spectrum, can be calculated by combining Eqs. 4 and 5.

For very low-conductivity solution ($\sigma_i \gg \sigma_e \gg \sigma_m$), use can be made of Eq. 6, which predicts the linear dependence of the characteristic frequency of the fastest antifield rotation (f_{c1}) on the external conductivity (Arnold and Zimmermann, 1988; Fuhr et al., 1996):

$$f_{cl} \cdot a = \frac{\sigma_e}{\pi \cdot C_m} + \frac{a \cdot G_m}{2\pi \cdot C_m} \tag{6}$$

According to Eq. 6, the characteristic frequency, f_{c1}, shifts linearly to higher frequencies with increasing external conductivity. Therefore, a plot of the frequency f_{c1} (normalized against radius) versus the external conductivity, σ_e, should yield a straight line and can be used for extracting the plasma membrane parameters, C_m and G_m.

Single-shell model with dispersive cytosol (model 2)

A reasonable agreement between the rotation theory and the experimental spectra observed over a wide range of the external conductivity was achieved if control Sp2 cells were modeled as single-shelled particles with a dispersion of the cytosol. The dispersive properties of the cytosol were described by Eq. 7 (Pethig and Kell, 1987; Schwan, 1988; Gimsa et al., 1996):

$$\epsilon_i^* = \epsilon_{ih} + \frac{\epsilon_{il} - \epsilon_{ih}}{1 + j\omega\tau_d} + \frac{\sigma_{il}}{j\omega} \tag{7}$$

where ϵ_{ih} (σ_{ih}) and ϵ_{il} (σ_{il}) are the values of the permittivity (conductivity) at high (subscript h) and low (subscript l) frequencies, $\tau_d = (2\pi f_d)^{-1}$ is the relaxation time, and f_d is the characteristic frequency of the dispersion.

Mobile charge model (model 3)

Models 1 and 2 were not applicable for fitting electrorotation spectra of Sp2 cells treated with most lipophilic anions tested here, because these models could not explain the appearance of an additional antifield rotational peak in the low-frequency range. Therefore we extended models 1 and 2 to the case of a membrane containing mobile charges (model 3). In model 3 the complex capacitance, C_m^*, of the plasma membrane is given by Eq. 8:

$$C_m^* = C_{mh} + \frac{C_{ml} - C_{mh}}{1 + j\omega\tau_{mc}} + \frac{G_{ml}}{j\omega} \tag{8}$$

where C_{mh} and C_{ml} are the high-frequency ("geometrical") and the low-frequency specific capacity [F m^{-2}] of the plasma membrane, respectively; G_{ml} is the low-frequency membrane conductivity [S m^{-2}]; and τ_{mc} is the time constant of the dielectric dispersion arising from the mobile charge within the membrane. The dispersion is centered at the characteristic frequency $f_{mc} = (2\pi\tau_{mc})^{-1}$. Equation 8 is based on the analysis given by Ketterer et al. (1971), who showed that adsorption of lipophilic ions to a lipid bilayer can result in a dielectric dispersion of the membrane properties. The magnitude, $\Delta C_m = C_{ml} - C_{mh}$, the characteristic frequency (f_{mc}), and the time constant (τ_{mc}) of the dispersion depend on the area specific concentration, N_t, and the translocation rate, k_i, of the adsorbed ion as follows: $\Delta C_m = N_t F^2/(2RT)$ and $k_i = \pi f_{mc} = (2\tau_{mc})^{-1}$.

This work was supported by grants from the Deutsche Forschungsgemeinschaft (SCHE 209/17-1) to WAS and VLS; SFB 176, project B7, to RB; and SFB 176, project B5, to UZ.

REFERENCES

Andersen, O. S., S. Feldberg, H. Nakadomari, S. Levy, and S. McLaughlin. 1978. Electrostatic interactions among hydrophobic ions in lipid bilayer membranes. *Biophys. J.* 21:35–70.

Arnold, W. M., B. Wendt, U. Zimmermann, and R. Korenstein. 1985. Rotation of a single swollen thylakoid vesicle in a rotating electric field. Electrical properties of the photosynthetic membrane and their modification by ionophores, lipophilic ions and pH. *Biochim. Biophys. Acta.* 813:117–131.

Arnold, W. M., and U. Zimmermann. 1982. Rotating-field-induced rotation and measurement of the membrane capacitance of single mesophyll cells of *Avena sativa. Z. Naturforsch.* 37c:908–915.

Arnold, W. M., and U. Zimmermann. 1988. Electro-rotation: development of a technique for dielectric measurements on individual cells and particles. *J. Electrostatics.* 21:151–191.

Arnold, W. M., U. Zimmermann, W. Heiden, and J. Ahlers. 1988. The influence of tetraphenylborates (hydrophobic anions) on yeast cell electro-rotation. *Biochim. Biophys. Acta.* 942:96–106.

Becker, F. F., X.-B. Wang, Y. Huang, R. Pethig, J. Vykoukal, and P. R. C. Gascoyne. 1995. Separation of human breast cancer cells from blood by differential dielectric affinity. *Proc. Natl. Acad. Sci. USA.* 92:860–864.

Benz, R. 1988. Structural requirement for the rapid movement of charged molecules across membranes. Experiments with tetraphenylborate analogues. *Biophys. J.* 54:25–33.

Benz, R., and F. Conti. 1981. Structure of the squid axon membrane as derived from charge-pulse relaxation studies in the presence of absorbed lipophilic ions. *J. Membr. Biol.* 59:91–104.

Benz, R., F. Conti, and R. Fioravanti. 1984. Extrinsic charge movement in the squid axon membrane. Effect of pressure and temperature. *Eur. Biophys. J.* 11:51–59.

Benz, R., P. Läuger, and K. Janko. 1976. Transport kinetics of hydrophobic ions in lipid bilayer membranes. Charge-pulse relaxation studies. *Biochim. Biophys. Acta.* 455:701–720.

Benz, R., and W. Nonner. 1981. Structure of the axolemma of frog myelinated nerve: relaxation experiments with a lipophilic probe ion. *J. Membr. Biol.* 59:127–134.

Benz, R., and U. Zimmermann. 1983. Evidence for the presence of mobile charges in the cell membrane of *Valonia utricularis. Biophys. J.* 43: 13–26.

Buchner, W., and W. A. Schenk. 1984. ^{13}C-NMR spectra of monosubstituted tungsten carbonyl complexes. The NMR *trans* influence in octahedral tungsten(0) compounds. *Inorg. Chem.* 23:132–137.

Bühler, R., W. Stürmer, H.-J. Apell, and P. Läuger. 1991. Charge translocation by the Na,K-pump. I. Kinetics of local field changes studied by

time-resolved fluorescence measurements. *J. Membr. Biol.* 121: 141–161.

Cafiso, D. S., and W. L. Hubbell. 1982. Transmembrane electrical currents of spin-labeled hydrophobic ions. *Biophys. J.* 39:263–272.

Demura, M., N. Kamo, and Y. Kobatake. 1985. Determination of membrane potential with lipophilic cations: correction of probe binding. *Biochim. Biophys. Acta.* 820:207–215.

Dilger, J. P., and R. Benz. 1985. Optical and electrical properties of thin monoolein lipid bilayers. *J. Membr. Biol.* 85:181–189.

Flewelling, R. F., and W. L. Hubbell. 1986. Hydrophobic ion interactions with membranes. Thermodynamic analysis of tetraphenylphosphonium binding to vesicles. *Biophys. J.* 49:531–540.

Fuhr, G., U. Zimmermann, and S. G. Shirley. 1996. Cell motion in time-varying fields: principles and potential. *In* Electromanipulation of Cells. U. Zimmermann and G. Neil, editors. CRC Press, Boca Raton, FL. 259–328.

Gascoyne, P. R. C., F. F. Becker, and X.-B. Wang. 1995. Numerical analysis of the influence of experimental conditions on the accuracy of dielectric parameters derived from electrorotation measurements. *Bioelectrochem. Bioenerg.* 36:115–125.

Gimsa, J., T. Müller, Th. Schnelle, and G. Fuhr. 1996. Dielectric spectroscopy of single human erythrocytes at physiological ionic strengh: dispersion of the cytoplasm. *Biophys. J.* 71:495–506.

Gröhn, P., G. Klöck, J. Schmitt, U. Zimmermann., A. Horcher, R. G. Bretzel, B. J. Hering, D. Brandhorst, H. Brandhorst, T. Zekorn, and K. Federlin. 1994. Large-scale production of Ba^{2+}-alginate-coated islets of Langerhans for immunoisolation. *Exp. Clin. Endocrinol.* 102:380–387.

Hladky, S. B. 1992. Kinetic analysis of lipid soluble ions and carriers. *Q. Rev. Biophys.* 25:459–475.

Hölzel, R. 1997. Electrorotation of single yeast cells at frequencies between 100 Hz and 1.6 GHz. *Biophys. J.* 73:1103–1109.

Honold, K., and G. Stark. 1984. Phase transition and lateral phase separation in planar membranes as sensed by the lipophilic ion dipicrylamine. *Biochim. Biophys. Acta.* 778:602–611.

Jones, T. B. 1995. Electromechanics of Particles. Cambridge University Press, New York.

Ketterer, B., B. Neumcke, and P. Läuger. 1971. Transport mechanism of hydrophobic ions through lipid bilayer membranes. *J. Membr. Biol.* 5:225–245.

King, R. B. 1967. Reactions of alkali metal derivatives of metal carbonyls. VIII. Preparation, protonation, and alkylation of sodium cyanopentacarbonylmetalates. *Inorg. Chem.* 6:25–29.

Klodos, I., N. U. Fedosova, and L. Plesner. 1995. Influence of intramembrane electric charge on Na,K-ATPase. *J. Biol. Chem.* 270:4244–4254.

Läuger, P., R. Benz, G. Stark, E. Bamberg, P. C. Jordan, A. Fahr, and W. Brock. 1981. Relaxation studies of ion transport systems in lipid bilayer membranes. *Q. Rev. Biophys.* 14:513–598.

Lebedev, A. V., and L. L. Boguslavsky. 1971. Experimental study of conduction mechanism of artificial phospholipid membranes by impedance measurements. *Biophysika.* 17:221–229 (in Russian).

Lichtenberg, H. C., H. Giebeler, and M. Höfer. 1988. Measurements of electrical potential differences across yeast plasma membranes with microelectrodes are consistent with values from steady-state distribution of tetraphenylphosphonium in *Pichia humboldii. J. Membr. Biol.* 103: 255–261.

Lu, C. C., A. Kabakov, V. S. Markin, S. Mager, G. A. Frazier, and D. W. Hilgemann. 1995. Membrane transport mechanisms probed by capacitance measurements with megahertz voltage clamp. *Proc. Natl. Acad. Sci. USA.* 92:11220–11224.

Luxnat, M., H.-J. Müller, and H.-J. Galla. 1984. Membrane solubility of chlorpromazine. Hygroscopic desorption and centrifugation methods yield comparable results. *Biochem. J.* 224:1023–1026.

Lynch, P. T., and M. R. Davey. 1996. Electrical Manipulation of Cells. Chapman and Hall, New York.

Nielsen, K., W. A. Schenk, M. Kriegmeier, V. L. Sukhorukov, and U. Zimmermann. 1996. Absorption of tungsten carbonyl anions into the lipid bilayer membrane of mouse myeloma cells. *Inorg. Chem.* 35: 5762–5763.

Nolan, D. P., and H. P. Voorheis. 1991. The distribution of permeant ions demonstrate the presence of at least two distinct electrical gradients in bloodstream forms of *Trympanosoma brucei. Eur. J. Biochem.* 202: 411–420.

Oberhauser, A. F., and J. M. Fernandez. 1995. Hydrophobic ions amplify the capacitive currents used to measure exocytotic fusion. *Biophys. J.* 69:451–459.

Pastushenko, V. Ph., P. I. Kuzmin, and Yu. A. Chizmadzhev. 1985. Dielectrophoresis and electrorotation—a unified theory of spherically symmetrical cells. *Studia Biophys.* 110:51–57.

Pauly, H., and H. P. Schwan. 1959. Über die Impedanz einer Suspension von kugelförmigen Teilchen mit einer Schale. Ein Modell für das dielektrische Verhalten von Zellsuspensionen und von Proteinlösungen. *Z. Naturforsch.* 14b:125–131.

Pethig, R., and D. B. Kell. 1987. The passive electrical properties of biological systems: the significance in physiology, biophysics and biotechnology. *Phys. Med. Biol.* 32:933–977.

Pickar, A. D., and R. Benz. 1978. Transport of oppositely charged lipophilic probe ions in lipid bilayer membranes having various structures. *J. Membr. Biol.* 44:353–376.

Pickar, A. D., and W. C. Brown. 1983. Capacitance of bilayers in the presence of lipophilic ions. *Biochim. Biophys. Acta.* 733:181–185.

Ruff, J. K. 1969. The chemistry of dinuclear carbonyl anions. IV. Thiocyanate- and cyanide-bridged complexes. *Inorg. Chem.* 8:86–89.

Schnelle, T., T. Müller, S. Fiedler, S. G. Shirley, K. Ludwig, A. Herrmann, G. Fuhr, B. Wagner, and U. Zimmermann. 1996. Trapping of viruses in high-frequency electric field cages. *Naturwissenschaften.* 83:172–176.

Schwan, H. P. 1988. Dielectric spectroscopy and electro-rotation of biological cells. *Ferroelectrics.* 86:205–233.

Scudiero, D. A., R. H. Schoemaker, J. D. Paull, A. Monks, S. Tierney, T. H. Hofziger, M. J. Currens, D. Seniff, and M. R. Boyd. 1988. Evaluation of soluble tetrazolium/formazan assay for cell growth and drug sensitivity in culture using human and other cell lines. *Cancer Res.* 48:4827–4833.

Smetjek, P., and S. Wang. 1991. Domains and anomalous adsorption isotherms of dipalmitoylphosphatidylcholine membranes and lipophilic ions: pentachlorophenolate, tetraphenylborate, and dipicrylamine. *Biophys. J.* 59:1064–1073.

Strohmeier, W., and K. Gerlach. 1961. Zum Reaktionsmechanismus der photochemischen Bildung von Pentacarbonylmetallverbindungen $M(CO)_5D$. *Chem. Ber.* 94:398–406.

Sukhorukov, V. L., W. M. Arnold, and U. Zimmermann. 1993. Hypotonically induced changes in the plasma membrane of cultured mammalian cells. *J. Membr. Biol.* 132:27–40.

Sukhorukov, V. L., C. S. Djuzenova, W. M. Arnold, and U. Zimmermann. 1994. DNA, protein and plasma-membrane incorporation by arrested mammalian cells. *J. Membr. Biol.* 142:77–92.

Sukhorukov, V. L., C. S. Djuzenova, H. Frank, W. M. Arnold, and U. Zimmermann. 1995. Electropermeabilization and fluorescent tracer exchange: the role of whole cell capacitance. *Cytometry.* 21:230–240.

Sukhorukov, V. L., and U. Zimmermann. 1996. Electrorotation of erythrocytes treated with dipicrylamine: mobile charges within the membrane show their "signature" in rotational spectra. *J. Membr. Biol.* 153: 161–169.

Turin, L., P. Béhé, I. Plonsky, and A. Dunina-Barkovskaya. 1991. Hydrophobic ion transfer between membranes of adjacent hepatocytes: a possible probe of tight junction structure. *Proc. Natl. Acad. Sci. USA.* 88:9365–9369.

Wang, X.-B., Y. Huang, P. R. C. Gascoyne, F. F. Becker, R. Hölzel, and R. Pethig. 1994a. Changes in Friend murine erythroleukaemia cell membranes during induced differentiation determined by electrorotation. *Biochim. Biophys. Acta.* 1193:330–344.

Wang, J., I. Spiess, C. Ryser, and U. Zimmermann. 1997a. Separate determination of the electrical properties of the tonoplasts and the plasmalemma of the giant-celled alga *Valonia utricularis*: vacuolar perfusion of turgescent cells with nystatin and other agents. *J. Membr. Biol.* 157:311–321.

Wang, J., V. L. Sukhorukov, C. S. Djuzenova, and U. Zimmermann. 1997b. Protoplasts of the giant marine alga *Valonia utricularis*: electrical and membrane transport properties measured by electrorotation. *Protoplasma.* 196:123–134.

Wang, J., U. Zimmermann, and R. Benz. 1994b. Contribution of electrogenic ion transport to impedance of the algae *Valonia utricularis* and artificial membranes. *Biophys. J.* 67:1582–1593.

Wolfram, S. 1996. The Mathematica Book, 3rd Ed. Wolfram Media, Champlain, IL.

Wulf, J., R. Benz, and G. W. Pohl. 1977. Properties of bilayer membranes in the presence of dipicrylamine. A comparative study by optical absorbtion and electrical relaxation measurements. *Biochim. Biophys. Acta.* 465:429–442.

Zimmermann, U., K.-H. Büchner, and R. Benz. 1982. Transport properties of mobile charges in algal membranes: influence of pH and turgor pressure. *J. Membr. Biol.* 67:183–197.

Zimmermann, U., and G. A. Neil. 1996. Electromanipulation of Cells. CRC Press, Boca Raton, FL.